


Review

Platinum Group Elements (PGE) Geochemistry and Mineralogy of Low Economic Potential (Rh-Pt-Pd)-Rich Chromitites from Ophiolite Complexes

Federica Zaccarini ^{1,*}, Maria Economou-Eliopoulos ², Olga Kiseleva ³, Giorgio Garuti ¹, Basilios Tsikouras ¹, Evgenii Pushkarev ⁴ and Arifudin Idrus ⁵

- ¹ Geosciences Programme, Faculty of Science, University Brunei Darussalam, Jalan Tungku Link, Gadong, Bandar Seri Begawan BE1410, Brunei
- ² Department of Geology and Geoenvironment, University of Athens, 15784 Athens, Greece
- ³ Sobolev Institute of Geology and Mineralogy, Siberian Branch of the Russian Academy of Sciences, 630090 Novosibirsk, Russia
- ⁴ Institute of Geology and Geochemistry, Ural Branch of the Russian Academy of Science, Vonsovskogo Str. 15, 620110 Yekaterinburg, Russia
- ⁵ Department of Geological Engineering, Universitas Gadjah Mada. Jl. Grafika 2 Bulaksumur, Yogyakarta 55281, Indonesia
- * Correspondence: federicazaccarinigaruti@gmail.com; Tel.: +43-664-386-8590



Citation: Zaccarini, F.; Economou-Eliopoulos, M.; Kiseleva, O.; Garuti, G.; Tsikouras, B.; Pushkarev, E.; Idrus, A. Platinum Group Elements (PGE) Geochemistry and Mineralogy of Low Economic Potential (Rh-Pt-Pd)-Rich Chromitites from Ophiolite Complexes. *Minerals* **2022**, *12*, 1565. <https://doi.org/10.3390/min12121565>

Academic Editors: Sytle M. Antao, Jennifer Kung and Nalini G. Sundaram

Received: 15 November 2022

Accepted: 2 December 2022

Published: 5 December 2022

Publisher's Note: MDPI stays neutral with regard to jurisdictional claims in published maps and institutional affiliations.



Copyright: © 2022 by the authors. Licensee MDPI, Basel, Switzerland. This article is an open access article distributed under the terms and conditions of the Creative Commons Attribution (CC BY) license (<https://creativecommons.org/licenses/by/4.0/>).

Abstract: This contribution provides an overview of platinum group elements (PGE) distribution and mineralogy in ophiolitic chromitites, which are unusually enriched in the low melting-point Rh, Pt and Pd (PPGE) compared with most chromite deposits associated with ophiolites, which are dominated by the refractory Os, Ir and Ru (IPGE). The PPGE-rich chromitites examined in this paper have a PPGE/IPGE ratio equal to or higher than 1 and represent about 7% of the ophiolitic chromitite population. These chromitites occur in the mantle unit, in the mantle-transition zone (MTZ), as well as in the supra-Moho cumulate sequence of ophiolite complexes. The age of their host ophiolites varies from Proterozoic to Eocene and, based on their composition, the chromitites can be classified into Cr-rich and Al-rich categories. Mineralogical assemblages observed in this investigation suggest that the PPGE enrichment was achieved in the magmatic stage thanks to the formation of an immiscible sulfide liquid segregating during or immediately after chromite precipitation. The sulfide liquid collected the available chalcophile PPGE that precipitated as specific phases together with Ni-Cu-Fe sulfides in the host chromitite and the silicate matrix. After their magmatic precipitation, the PPGM and associated sulfides were altered during low-temperature serpentinization and hydrothermal processes. Therefore, the original high-temperature assemblage underwent desulfurization, generating awaruite and alloys characterized by variable Pt-Pd-Rh-Cu-Ni-Fe assemblages. The occurrence of secondary PPGM containing Sb, As, Bi, Te, Sn, Hg, Pb and Au suggests that these elements might have been originally present in the differentiating magmatic sulfide liquid or, alternatively, they were introduced by an external source transported by hydrothermal and hydrous fluids during the low-temperature evolution of the host ophiolite. Although the PGE content may be as high as 81,867 ppb, as was found in one sample from Shetland chromite deposits, the ophiolitic chromitites are presently considered as a potential resource because of the following circumstances: (1) enrichment of PPGE in podiform chromitites is a local event that occurs randomly in ophiolite sequences, (2) ore deposits are small and characterized by uneven distribution and high discontinuity, (3) physical characters of the mineralization only allow poor recovery of the precious metals mainly due to the minute grain size, and (4) for these reasons, the PPGE reserves in ophiolitic chromitites cannot compete, at the moment, with those in chromite deposits of the Bushveld type that will supply world demands for centuries using current mining techniques.

Keywords: chromitite; ophiolite; platinum group elements; platinum group minerals

1. Introduction

Platinum (Pt), palladium (Pd), rhodium (Rh), iridium (Ir), ruthenium (Ru) and osmium (Os) are known as the platinum group elements (PGE). These metals are characterized by peculiar physical and chemical properties, such as high melting points, resistance to oxidation and corrosion, strong conductivity and ductility [1,2]. Among the PGE, platinum and palladium have gained a great economic importance due to their use in oil refining, electronics, jewelry, the glass industry, medical applications and in the catalytic converter of vehicles to reduce the pollutants of exhaust gases [1–3]. Therefore, PGE and in particular platinum and palladium mine production have grown continuously since the second world war in response to the development of their modern applications.

Furthermore, considering the transformation towards a greener economy that started a few years ago and that PGE uses play an important role in reducing greenhouse gases, their price has increased rapidly [2]. The PGE are among the less abundant elements in the Earth [2]. However, local high PGE contents can be achieved through a combination of complex geochemical and geological processes that, in some cases, result in the formation of economic deposits [1,4]. Based on their geochemical behavior, the PGE have been divided in two subgroups: the Ir-subgroup (IPGE) consisting of Os, Ir and Ru and the Pd-subgroup (PPGE) consisting of Rh, Pt and Pd [5]. The IPGE are more refractory and less chalcophile than the PPGE. Therefore, the IPGE are more concentrated in chromitite, while PPGE tend to follow the sulfides [4]. For many decades, both the podiform and stratiform chromitites have been recognized as efficient collectors of the critical PGE. Chromitites start to precipitate at temperatures well above 1000 °C; therefore, most of them are enriched in the refractory IPGE, showing contents several orders of magnitude higher than their peridotites. Few chromitites contain economic amounts of the more valuable PPGE, such as the Upper Group 2 (UG2) stratiform chromitites of the Bushveld layered intrusion of South Africa, that still represent the only example of chromitite mined for the PGE recovery [1].

Additionally, the chromitites associated with the Ural–Alaskan concentrically zoned complexes are enriched in Pt and contain a great number of Pt-bearing minerals but, despite this enrichment, few of them are mined for the PGE recovery due to the small size of the mineralized bodies [6].

Two different types of chromitite have been reported within the ophiolites: (1) podiform chromitite that generally occurs in the mantle tectonite and (2) layered chromitite hosted at the base of supra-Moho cumulates, above the crustal sequence. About half a century ago, the podiform chromitites hosted in the mantle section of ophiolite complexes attracted the attention of economic geologists as a potential target for PGE recovery [7]. Several studies have shown that the majority of the ophiolitic chromitites are enriched in the refractory IPGE, and only a few of them show anomalous contents of the most economically significant PPGE.

It is generally agreed that the PGE enrichment in the podiform chromitites is due to the presence of the so-called platinum group minerals (PGM) that occur as tiny grains enclosed in the chromite crystals and, to a lesser extent, in the silicates of the chromitite matrix [8–23]. This observation has promoted investigation of the chromitites in order to verify the mineralogical nature, size, morphology and textural position of PGM, with the aim to understand their origin and to provide useful information for their beneficiation during mineral processing. Consistently with their geochemical signature, the most abundant PGM described in the podiform chromitites consist of IPGE-minerals (IPGM), such as sulfides of the laurite–erlichmanite series, alloys in the Os–Ir–Ru system and sulfarsenides of Ir, Ru and Os [8–23]. The few ophiolitic chromitites enriched in Rh, Pt and Pd were also proved to contain abundant and complex PPGE minerals (PPGM). The main target of this contribution is to provide an overview of unpublished and existing data from the few ophiolitic chromitites enriched in PPGE and PPGM, in order to evaluate their economic potential. Their PGE geochemical and mineralogical aspects are discussed and combined with the chromite composition of their host chromitites, with the aim to understand the processes that caused their anomalous enrichment in PPGE and PPGM.

2. Worldwide Occurrence of PPGE-Rich Ophiolitic Chromitites

After a careful revision of a huge set of the available literature, it was possible to establish that only 7% of ophiolitic chromitites display enrichment in PPGE over IPGE, reflecting overabundance of specific PPGM. In this review we have selected chromitites characterized by the PPGE-IPGE ratio equal to or higher than 1, regardless of the total PGE content, and those that contain abundant PPGM (Table 1 and references therein).

A few examples representing PPGE- and PPGM-rich ophiolitic chromitites have been reported from Canada and the USA [24–27], from the Caribbean area [21,28–30], from North, West and Central Europe [10,11,18,22,23,31–48], from Cyprus [9], from Turkey and Saudi Arabia [49,50], from Urals and East Sayan of Russia [51–57], and from The Philippines, Indonesia and New Caledonia [12,13,58,59] (Figure 1). Detailed information regarding the geographical location, name and age of the host ophiolite and deposits, chromite composition, stratigraphic position and data available of the chromitites overviewed in this work are provided in Table 1.

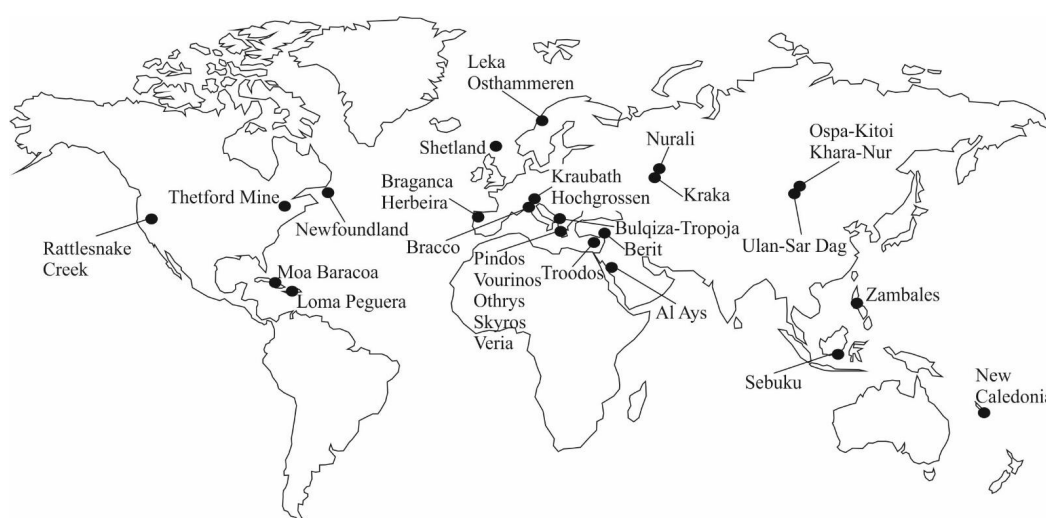


Figure 1. World-wide distribution of the PPGE-PPGM-rich ophiolitic chromitites.

Most of the chromitites have been analyzed for the PGE distribution and for the presence of PGM. According to Table 1, PPGE-PPGM-rich chromitites have been reported from 19 countries of the northern hemisphere (Figure 1), except for Indonesia and New Caledonia, which belong to the southern hemisphere. Geochronological data show a variation range from Proterozoic to Eocene. On the basis of the ideal stratigraphy of the host ophiolite, the PPGE-PPGM-rich chromitites occur in the mantle, in the mantle transition zone (MTZ) and in the cumulus pile of the crustal sequence (Table 1). From a compositional point of view, the ophiolitic chromitites are classified as Cr-rich ($Cr\# = Cr/(Cr + Al) > 0.7$) and Al-rich ($Cr\# < 0.7$) [60]. Considering this classification, the PPGE-PPGM-rich ophiolitic chromitites have been described in both the Cr-rich and Al-rich categories. Major Cr-rich chromitites occur in the mantle sequence of Kraubath and Hochgrossen (Austria), Newfoundland (Canada), Loma Caribe (Dominican Republic), Veria (Greece), Ospa-Kitoi, Khara-Nur and Ulan-Sar'dag (Russia), Herbeira (Spain) and Shetland (UK) ophiolites (Table 1 and references therein). Al-rich chromitites rarely occur in the mantle unit and have been reported only in Skyros, Pindos and Othrys (Greece) ophiolites (Table 1 and references therein). In the MTZ, only the presence of Al-rich chromitites has been documented such as in the Moa Baracoa (Cuba), Nurali (Russia) and Berit (Turkey) ophiolites. The cumulus pile, above the Moho, contains Al-rich chromitites in the ophiolites of Bracco (Italy), Sebuk (Indonesia) and New Caledonia, as well as Cr-rich chromitites in the ophiolites of Thetford Mine (Canada), Troodos (Cyprus), Zambales (The Philippines) and Al'Ays (Saudi Arabia) [8,11–13,18,24–50].

Table 1. World-wide occurrences of PPGE-PPGM-rich ophiolitic chromitites (listed in alphabetical order according to the host country).

Country	Ophiolite	Name of the Deposit	Age	Type of Chromitite	Chromite Composition	PPGE Data *	PPGM Data	Ref.
Albania	Bulquiza-Tropoja		Jurassic	mantle-cumulate	n.a.	no	yes	[18]
Austria	Kraubath		Early Paleozoic	mantle	Cr-rich	yes	yes	[11,36]
	Hochgrossen		Early Paleozoic	mantle	Cr-rich	yes	no	[11]
Canada	Newfoundland	Middle Arm Brook	Lower Ordovician	mantle	Cr-rich	yes	yes	[26]
	Thetford Mine		Lower Ordovician	cumulate	Cr-rich	yes	yes	[24,25]
Cuba	Moa Baracoa	Potosi	Upper Jurassic-Lower Cretaceous	MTZ	Al-rich	yes	yes	[28,29]
Cyprus	Troodos		Cretaceous	cumulate	Cr-rich	yes	no	[9]
Dominican Republic	Loma Caribe	Loma Peguera	Jurassic-Cretaceous	mantle	Cr-rich	no	yes	[21,30]
Greece	Pindos	Korydallos, Pefki	Middle-Upper Jurassic	mantle	Al-rich	yes	yes	[42–47]
	Vourinos	Pefka, Rodiani	Jurassic-Cretaceous	mantle	Cr-rich	yes	no	[39]
	Otrhys	Eretria-Tsangli	Jurassic-Cretaceous	mantle	Al-rich	yes	yes	[44,48]
		Aghios Stefanos						
	Skyros Island	Achladones	Jurassic-Cretaceous	mantle	Alr-rich	yes	yes	[41,44]
	Veria	Galaktos	Jurassic-Cretaceous	mantle	Cr-rich	yes	yes	[22,23]
Italy	Bracco	Ziona, Cima Stronzi, Canegreca, Mattarana, Pian della Madonna,	Jurassic	mantle-cumulate	Al-rich	yes	no	[38]
Indonesia	Sebuku Island		Jurassic-Cretaceous	mantle-cumulate	Al-rich	no	yes	[59]
New Caledonia	New Caledonia	Pirogue	Cretaceous-Paleocene	cumulate	Al-rich	yes	yes	[12,13]
Norway	Leka		Lower Ordovician	mantle-cumulate	n.a.	yes	yes	[33]
	Osthammeren		Lower Ordovician	mantle	n.a.	no	yes	[10]
Philippine	Zambales	Acoje	Eocene	cumulate	Cr-rich	yes	no	[58]
Portugal	Braganca	Derruida	Paleozoic	n.a.	n.a.	yes	yes	[32]
Russia	Nurali	CHR II	Paleozoic	MTZ	Al-rich	yes	yes	[51–53]
	Ospa-Kitoi		Proterozoic	mantle	Cr-rich	yes	yes	[54,55]
	Khara-Nur		Proterozoic	mantle	Cr-rich	yes	yes	[54,55]
	Ulan-Sar'dag		Neoproterozoic	mantle	Cr-rich	yes	no	[56]
	Kraka	Wets Saksey, Loginovskoe, Babay	Paleozoic	cumulate	Cr-rich	yes	yes	[57]
		East Saksey, Laktybash, Khamitovskoe, Maly Apshak, Bol'shoy Apshak		mantle	Al-Cr-rich	yes	yes	
Saudi Arabia	Al'Ays		n.a.	mantle-cumulate	Cr-rich	yes	yes	[50]
Spain	Herbeira		Paleozoic	mantle	Cr-rich	yes	yes	[35,37]
Turkey	Berit		Cretaceous	MTZ	Al-rich	yes	yes	[49]
United Kingdom	Shetland	Harold's Grave Cliff	Early Paleozoic	mantle	Cr-rich	yes	yes	[31,34]
USA	Rattlesnake Creek	Pole Corral	n.a.	n.a.	n.a.	yes	no	[27]

* = published analyses with PPGE-IPGE ratio equal to or higher than 1; n.a. = not available; Ref. = References.

3. PGE Geochemistry

Whole-rock PGE analyses of 123 ophiolitic chromitites with PPGE/IPGE \Rightarrow 1 are listed in Table 2.

Table 2. Whole-rock PGE analyses (ppb) of ophiolitic chromitites with PPGE-IPGE ratios equal to or higher than 1.

	Os	Ir	Ru	Rh	Pt	Pd	Σ PGE	PPGE/IPGE	Ref.
AUSTRIA									
Hochgrossen	109	149	287	85	446	22	1098	1	[11,36]
Hochgrossen	250	310	620	130	940	390	2640	1	
Kraubath	34	52	120	98	470	390	1164	5	[36]
Kraubath	160	80	220	110	250	370	1190	2	
CANADA									
Tetford Mines									[25]
Hall	268	308	566	121	2000	35	3298	2	
Finneth	33	44	130	280	1900	690	3077	14	[26]
Newfoundland									
White Hills		1	1	20	120	2	144	71	[26]
Middle Arm Brook	42	75	128	91	547	157	1040	3	
Middle Arm Brook	12	1	33	15	107	33	201	3	[28]
CUBA									
Potosi	188	115	234	38	291	247	1113	1	[28]
Potosi	99	57	79	22	172	69	498	1	
CYPRUS									
Troodos	6	29	140	49	79	69	372	1	[9]
GREECE									
Othrys									[44]
Othrys	70	36	97	11	256	3	473	1	
Othrys	8	12	16	8	189	9	242	6	[39,40]
Vourinos									
Pefka	10	8	17	5	142	440	622	17	[42–47]
Rodiani	23	6	25	8	275	108	445	7	
Pindos									[42–47]
Korydallos	62	47	80	112	1460	337	2098	10	
Korydallos	70	55	110	98	2220	766	3319	13	[42–47]
Korydallos	47	49	55	104	3020	600	3875	25	
Korydallos	14	11	57	13	3460	1660	5215	63	[42–47]
Korydallos	17	21	30	31	31	192	322	4	
Korydallos	266	364	2100	1140	17,100	7860	28,830	10	[42–47]
ITALY									
Bracco									[38]
Ziona	4	1	3	1	18	5	32	3	
Ziona	3	1	2	1	14	4	25	3	[38]
Ziona	3	0.1	1	1	12	2	19	4	
Ziona	3	0.1	1	1	10	2	17	3	[38]
Mt. San Nicolao	2	1	1	1	13	12	30	7	
Mt. San Nicolao	1	1	2	1	10	7	22	5	[38]
Mt. San Nicolao	4	1	3	4	23	29	64	7	
Mt. San Nicolao	3	1	2	3	23	35	67	11	[38]
Canegreca	3	1	3	5	25	35	72	10	
Mattarana	3	0.1	1	2	10	7	23	5	[38]
Mattarana	4	0.2	1	1	14	7	27	4	
Mattarana	11	1	4	4	46	13	78	4	[38]
Mattarana	9	0.5	3	5	38	13	68	4	
Mattarana	11	0.4	4	4	37	12	68	3	[38]
Mattarana	13	0.4	3	4	35	12	68	3	
Pian della Madonna	3	0.2	1	1	11	3	19	4	[38]
NEW CALEDONIA									
Pirogues	-	40	110	170	4610	550	5480	36	[13]
Pirogues	-	170	310	420	9810	470	11,180	22	
Pirogues	-	200	280	440	5940	430	7290	14	[13]
Pirogues	-	740	190	630	11,500	900	13,960	14	
Pirogues	-	90	70	90	3300	200	3750	22	[13]
NORWAY									
Leka	360	410	60	210	4600	2700	8340	9	[33]
Leka	180	240	370	150	2400	1600	4940	5	
Leka	340	220	56	150	1800	1200	3766	5	[33]
Leka	240	220	48	160	2100	960	3728	6	

Table 2. Cont.

	Os	Ir	Ru	Rh	Pt	Pd	Σ PGE	PPGE/IPGE	Ref.
Leka	210	210	40	140	1500	690	2790	5	
Leka	400	240	84	300	1000	550	2574	3	
Leka	270	170	64	210	1100	730	2544	4	
Leka	180	76	40	80	740	1400	2516	8	
Leka	370	250	96	270	1000	420	2406	2	
Leka	130	83	260	55	640	1000	2168	4	
Leka	58	44	120	39	440	670	1371	5	
PHILIPPINES									
Zambales	78	189	506	135	1417	1796	4121	4	[58]
Zambales	-	460	1100	759	5958	8351	16,628	10	
PORTUGAL									
Bragança	670	1600	1150	605	4050	3150	11,225	2	[32]
RUSSIA									
Nurali	97	80	42	130	5997	1396	7742	34	[51,53]
Nurali	40	111	62	263	8940	2190	11,606	53	
Nurali	34	60	74	72	979	231	1450	8	
Ulan-Sar'dag	45	26	68	12	39	177	367	2	[56]
Ulan-Sar'dag	51	58	53	10	49	182	403	1	
Ulan-Sar'dag	49	57	121	24	49	478	778	2	
Ulan-Sar'dag	37	20	59	16	64	97	293	2	
Ulan-Sar'dag	46	20	46	11	41	78	242	1	
Ulan-Sar'dag	7	6	20	21	35	903	992	29	
Khara-Nur	13	5	14	6	16	28	82	2	[54–56]
Khara-Nur	35	40	105	29	103	172	484	2	
Ospa-Kittoi	66	49	100	26	136	150	527	1	[54–56]
Ospa-Kittoi	110	190	180	20	490	360	1350	2	
Ospa-Kittoi	240	200	210	20	1240	890	2800	3	
Ospa-Kittoi	29	21	30	18	87	139	324	3	
Kraka	4	17	20	13	4	69	127	2	[57]
Kraka	3	24	62	28	8	154	278	2	
Kraka	5	47	20	47	2103	200	2422	33	
Kraka	59	104	215	52	429	295	1154	2	
Kraka	73	114	59	-	1737	5	1988	7	
Kraka	32	51	38	-	580	5	706	5	
Kraka	26	49	52	-	154	86	367	2	
Kraka	9	14	17	-	116	66	222	5	
SAUDI ARABIA									
Al'Ays	30	75	180	80	200	36	601	1	[50]
Al'Ays	42	130	220	150	470	83	1095	2	
Al'Ays	200	248	436	155	697	36	1772	1	
Al'Ays	142	173	333	111	494	165	1418	1	
Al'Ays	6	52	150	130	200	940	1478	6	
Al'Ays	24	50	130	58	310	1200	1772	8	
Al'Ays	14	22	41	45	81	100	303	3	
Al'Ays	54	55	73	26	69	220	497	2	
Al'Ays	41	152	430	147	720	340	1830	2	
Al'Ays	22	27	89	32	97	71	338	1	
Al'Ays	6	20	68	46	150	1000	1290	13	
Al'Ays	100	198	500	225	2570	6870	10,463	12	
SPAIN									
Herbeira									
C4-1	165	600	600	1100	7000	3900	13,365	9	[37]
C4-6	185	420	470	860	5600	4400	11,935	10	
C4-3	200	410	600	940	3700	2650	8500	6	
C4-4	86	260	290	480	4600	2550	8266	12	
H-17	68	285	235	460	3200	740	4988	7	
C4-5	34	58	70	112	1900	2750	4924	29	
H-24	52	190	190	380	1900	900	3612	7	
TURKEY									
Berit	-	8	19	10	2	10	48	5	[49]
Berit	28	62	108	271	143	271	883	12	
Berit	-	17	46	5	11	5	84	1	
Berit	-	3	9	10	3	10	35	10	
Berit	5	6	11	74	144	74	314	12	
Berit	41	25	35	1700	4469	1700	7970	55	
Berit	-	6	25	21	11	21	84	11	
Berit	-	7	16	25	31	25	104	13	
Berit	33	32	51	321	509	321	1267	18	

Table 2. Cont.

	Os	Ir	Ru	Rh	Pt	Pd	Σ PGE	PPGE/IPGE	Ref.
Berit	-	3	12	11	6	11	43	11	
Berit	39	38	52	1500	2385	1500	5514	54	
UK									
Shetland									
Cliff	1200	3200	4400	1500	28,000	35,000	73,300	7	[34]
Cliff	1400	2500	3100	1500	22,000	30,000	60,500	8	
Cliff	500	900	1300	480	9300	9900	22,380	7	
Cliff	370	600	970	330	5800	7300	15,370	7	
Cliff	-	3167	5733	1300	25,667	46,000	81,867	8	
Cliff	50	97	190	55	500	520	1412	3	
Cliff	34	83	170	69	370	180	906	2	
Harold's grave	800	1100	1800	220	370	3400	7690	1	
Quarry 12S	32	52	96	37	250	390	857	4	
Quarry 10	20	22	58	17	120	190	427	3	
USA									
Oregon California									
Rattlesnake Creek	-	190	280	36	1060	10	1576	2	[27]
Rattlesnake Creek	-	110	250	33	545	110	1048	2	
Rattlesnake Creek	-	20	100	14	120	34	288	1	

Ref. = References.

Most analyses report contents of all the six PGE, except samples from the USA, New Caledonia, Canada, The Philippines, Turkey and the UK, in which Os was not analyzed. In a few samples from Kraka, Russia, Rh was not reported. The distribution of PGE is not homogeneous, as the total PGE varied from a few ppb up to more than 80 ppm (Table 2 and reference therein). The lowest contents (13–100 ppb) were found in the Al-rich chromitites of the Bracco complex (Italy) [38] and in a few samples from the Al-rich chromitites of Berit (Turkey) [49]. The highest values (81,867 ppb) were found in Cr-rich chromitites of the Shetland ophiolite (UK) [34]. Figure 2A shows that 48% of the samples contain total PGE up to 1000 ppb, 15% from 1000 to 2000 ppb, 7% from 2000 to 3000 ppb, and from 3000 to 4000, 12% from 4000 to 10,000, 8% from 10,000 to 20,000 and only 3% contain more than 20,000. Enrichment in total PGE of up to more than 2000 ppb is found in both the Al-rich and Cr-rich chromitites, independently from stratigraphic position in the ophiolite sequence. The values of the PPGE/IPGE ratio vary greatly, from 1 to 71 (Figure 2B), regardless the chromitite composition or geological setting (mantle, transition zone, crustal sequence). A total of 69% of samples have a PPGE/IPGE ratio in the range 1–9 and 27% are in the range from 10 to 50 (Figure 2B). The highest ratios (50 to 71) are found in 4% of samples from the deposits of Berit [49], Pindos [43], Newfoundland [26] and Nurali [51], Table 2. The chondrite [61]-normalized PGE patterns of the available data from the investigated chromitites are illustrated in Figure 3A–P, using the data and their source reported in Table 2. The chromitites of Austria, Cuba and the USA display almost flat or saw-like patterns (Figure 3A,C,P). A few chromitites from Vourinos and Pindos (Figure 3E), Norway (Figure 3H), The Philippines (Figure 3I), Portugal (Figure 3J), Kraka (Figure 3K) and Saudi Arabia (Figure 3L) show positive sloping PGE patterns. The PGE profiles of the Turkish chromitites (Figure 3N) show PPGE enrichments which are dominated by a marked positive Rh anomaly. The Pt/Pd ratios vary greatly, between 0.1 and 106, resulting in markedly variable slopes in the chondrite-normalized spidegrams (Figure 3A–P). The plotted patterns show variable positive or negative slopes or they are nearly unfractionated with respect to Pt and Pd. In particular, all the chromitites from Canada, New Caledonia, Nurali (Russia), the USA and Greece (with the exception of one sample from Vourinos) show negative slopes (Figure 3B,E,G,K,P), whereas chromitites from Kraubath (Austria), Cyprus, The Philippines, Portugal, Ulan-Sar dag (Russia) and the majority of the samples from the UK (Figure 3A,D,I–K,O) demonstrate positive slopes between Pt and Pd. The chromitites from Cuba, Italy, Norway, Kraka (Russia), Saudi Arabia, Spain and Turkey are characterized by positive, negative and almost flat PGE patterns (Figure 3C,F,H,K–N).

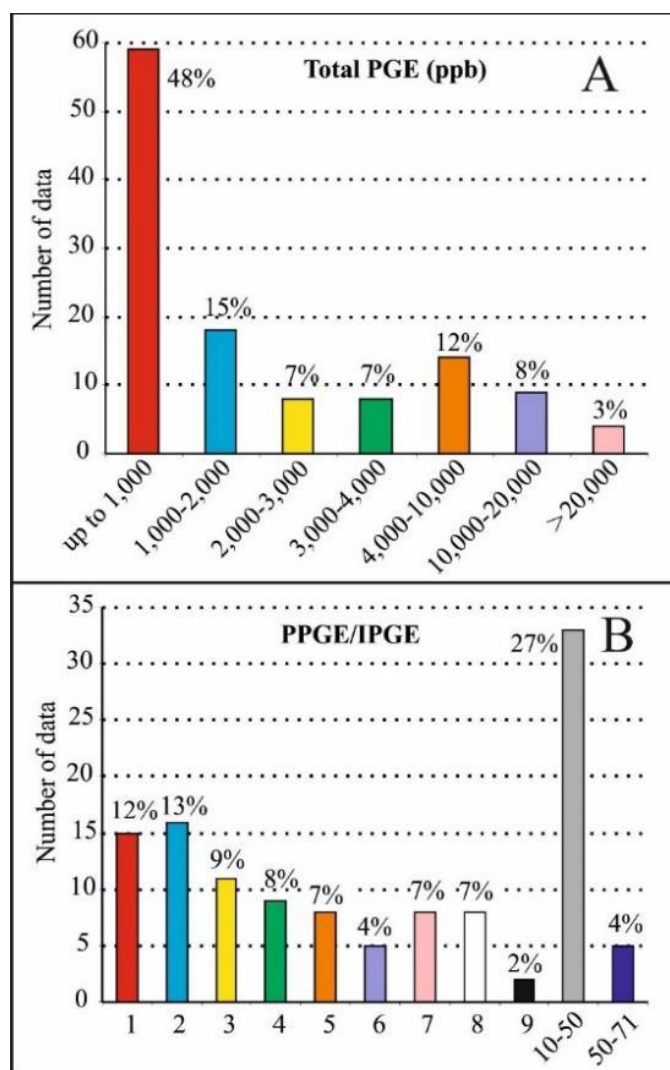


Figure 2. Statistical distribution of the PGE in the overviewed chromitites. (A) Total PGE abundance, (B) frequency of the values of the PPGE/IPGE ratio.

The PGE distributions in the overviewed chromitites, from which more than two analyses were available, were plotted in the binary diagram. Pt/Pt* versus Pd/Ir (Figure 4A) was used to discriminate residual mantle rocks from those characterized by a fractionation trend [61]. The values of Pt/Pt* refer to the so-called Pt anomaly and were calculated using the formula $Pt/Pt^* = Pt_N / \sqrt{(Rh_N \times Pd_N)}$, proposed by Garuti et al. [61]. The Pt anomaly provides a measure of the deviation of Pt from the general trend of the normalized PGE pattern of a sample. The Pt anomaly coupled with the Pd/Ir ratio in the analyzed samples can be used to define different petrological processes, such as fractionation and partial melting trends (Figure 4A).

The diagram shows that the analyzed chromitites are not consistent with mantle residuum after partial melting, but most of them roughly follow a general fractionation trend (Figure 4A).

The same data have been plotted in the diagram of Figure 4B proposed by Leblanc [7] to show that the PGE contents of the podiform chromitites in ophiolites increase with decreasing Pd/Ir ratios, suggesting that the high PGE contents mainly result from an enrichment of Ir relative to Pd. With a few exceptions that include analyses from Greece and Turkey, all the data of the PPGE-rich chromitites are not consistent with the classical mantle-hosted chromitites enriched in IPGE (Figure 4B).

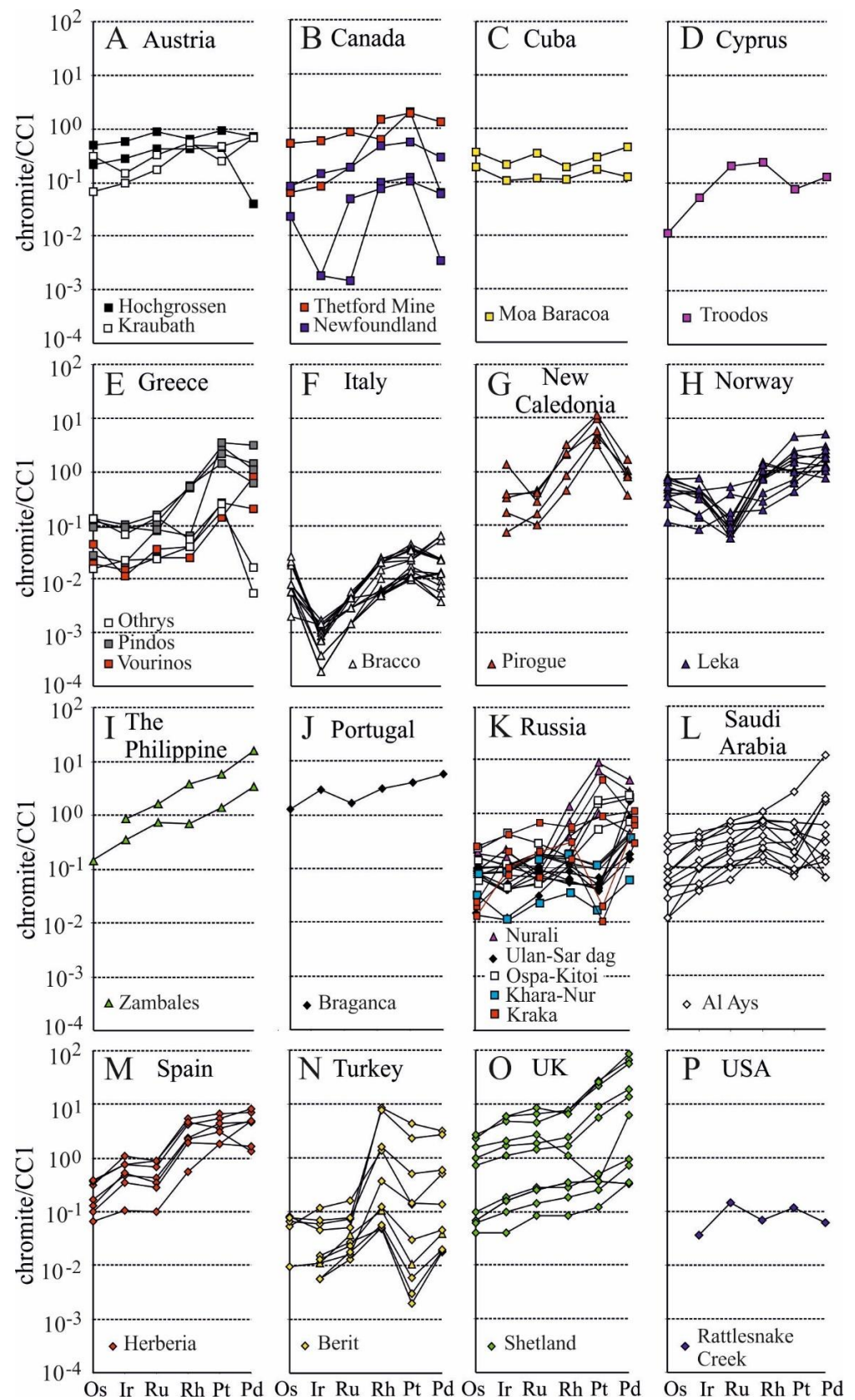


Figure 3. Chondrite [61]-normalized patterns of the overviewed chromitites, according to their geographical location. (A) Austria, (B) Canada, (C) Cuba, (D) Cyprus, (E) Greece, (F) Italy, (G) New Caledonia, (H) Norway, (I) The Philippines, (J) Portugal, (K) Russia, (L) Saudi Arabia, (M) Spain, (N) Turkey, (O) UK, (P) USA. See Table 2 for data source and references.

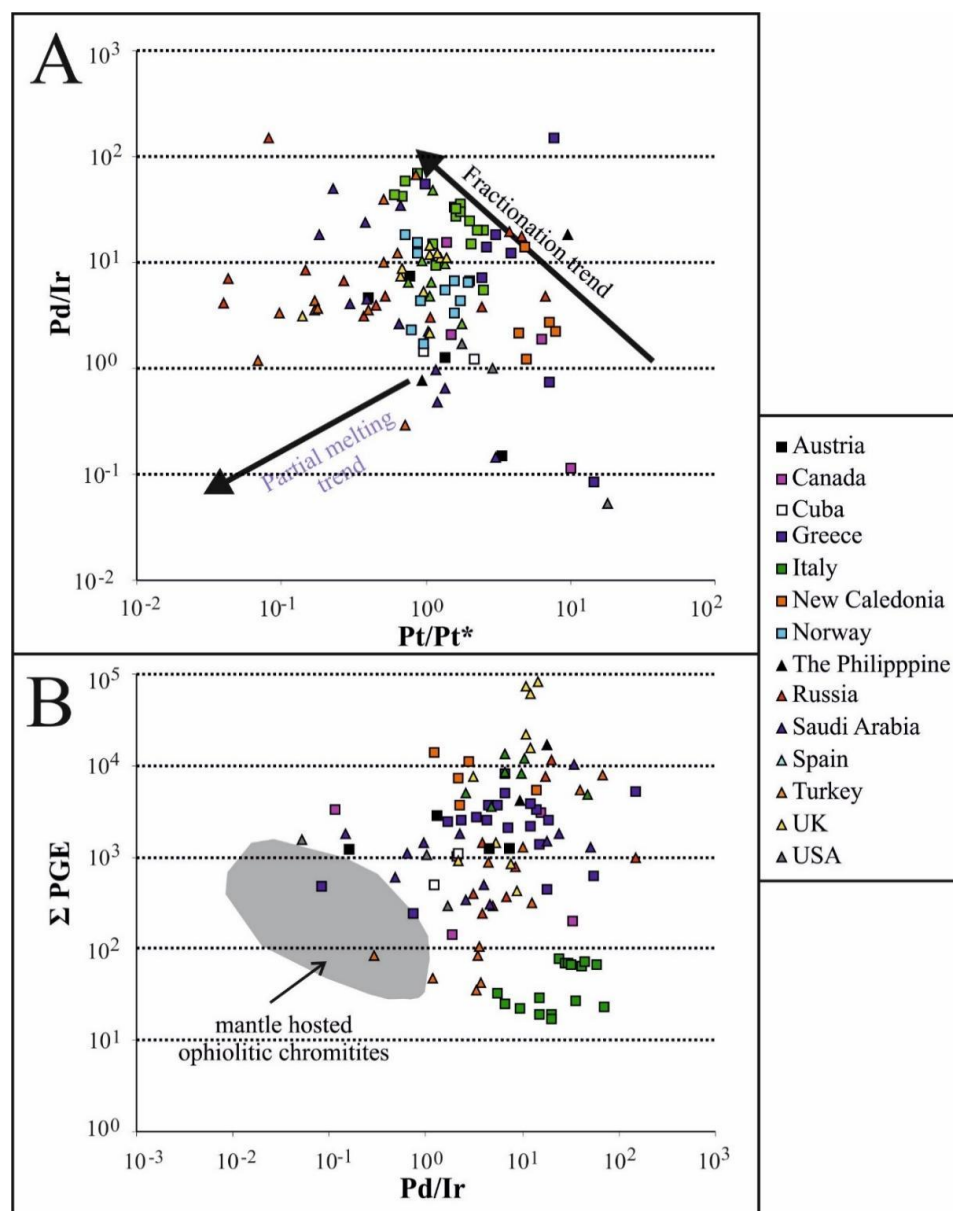


Figure 4. Binary diagrams for PPGE-rich ophiolitic chromitites. (A) Plot of the ratio Pd/Ir versus Pt/Pt* (calculated after Garuti et al. [62]), (B) PGE contents versus Pd/Ir ratio and comparison with the IPGE-rich ophiolitic chromitite, redrawn after Leblanc [7].

4. PGE Mineralogy

Consistent with the PGE geochemistry, besides the typical presence of IPGM such as sulfides of laurite-erlichmanite series, alloys of the Os-Ir-Ru system and irarsite, that generally occur as tiny grains less than 15 microns enclosed in the chromite crystals, several PPGM have been described in the PPGE-rich ophiolitic chromitites (Table 3 and references therein). The discovered PPGM are characterized by a great variety of mineralogical species, including 26 minerals approved by the Commission of New Minerals, Nomenclature, and Classification (CNMNC) of the International Mineralogical Association (IMA), 11 unnamed minerals with a composition that corresponds to possible new phases and 28 unidentified phases, for which a precise stoichiometry was not calculated (Table 3 and references therein). The coexistence of Rh, Pt and Pd minerals has been found in the chromitites of Bulqiza-Tropoja (Albania), Kraubath (Austria), Newfoundland and Thetford Mine (Canada), Osthhammeren (Norway), Braganca (Portugal), Al'Ays (Saudi Arabia), Herbeira (Spain) and Berit (Turkey) (Table 3).

Table 3. PPGM identified in the PPGE-enriched ophiolitic chromitites.

	1	2	3	4	5	6	7	8	9	10	11	12	13	14	15	16	17	18	19	20	21
Rhodium																					
Approved minerals																					
Bowieite Rh ₂ S ₃	x	x		x								x									
Cuprorhodsite CuRh ₂ S ₄	x	x		x								x									
Kingstonite Rh ₃ S ₄	x											x									
Hollingworthite RhAsS	x	x					x	x		x		x	x	x				x	x	x	x
Minakawaite RhSb												x						x			
Zaccariniite RhNiAs				x		x				x	x					x		x			
Unnamed minerals																					
RhTe	x																				
Rh ₂ As	x																				
Rh ₂ S ₃		x																			
Rh ₅ S ₄												x									
Rh ₂ SnCu				x												x					
Unidentified minerals *																					
Rh-Pd-Sb			x																		
Rh-As																		x			
	1	2	3	4	5	6	7	8	9	10	11	12	13	14	15	16	17	18	19	20	21
Platinum																					
Approved minerals																					
Braggite (Pt,Pd,Ni)S				x			x												x		
Cooperite (Pt,Pd,Ni)S	x			x				x				x			x		x				
Genkinite (Pt,Pd) ₄ Sb ₃																					x
Geversite Pt(Sb,Bi) ₂																x		x			
Hongshiite PtCu																					x
Isoferroplatinum Pt ₃ Fe	x			x								x				x					
Malanite CuPt ₂ S ₄	x			x								x									
Platarsite PtAsS	x	x						x		x			x	x							
Platinum Pt	x																				
Sperrylite PtAs ₂		x			x		x		x			x	x			x		x	x	x	x
Tetraferroplatinum PtFe	x			x												x			x		
Tulameenite Pt ₂ FeCu	x											x									
Unnamed minerals																					
Pt(Ni,Fe) ₃						x	x														
Pt ₆ Cu																		x			
Unidentified minerals *																					
Pt-Cu	x			x												x					
Pt-Pd-Cu														x		x					
Pt-Pd-Au																				x	
Pt-Pd-Cu-Au																					x
Pt-Fe-Cu												x		x			x				
Pt-Pd-Cu-Ni-Fe			x	x												x	x	x			
Pt-Fe		x					x		x			x	x			x				x	
Pt-Ir											x		x			x				x	
Pt-Ir-Fe-Ni						x															
Pt-Ru-Rh												x									
Pt-Ir-Ru-Os																x					
Pt-Pd-S																x					
Pt-Pd-Rh																		x			
Pt-oxides												x				x		x			
Cu-Pt oxides																				x	
	1	2	3	4	5	6	7	8	9	10	11	12	13	14	15	16	17	18	19	20	21
Palladium																					
Approved minerals																					
Atheneite (Pd,Hg,Pt) ₃ As														x							
Cabriiite Pd ₂ SnCu				x																	
Froodite PdBi ₂														x							
Keithconnite Pd _{3-x} Te	x	x																			
Mertierite II Pd ₈ (Sb,As) ₃		x																			
Nielsenite PdCu ₃							x														
Paolovite Pd ₂ Sn							x														
Plumbopalladinite Pd ₃ Pb ₂																	x				
Potarite PdHg	x	x												x		x			x		x
Skaergaarite PdCu							x														

Table 3. Cont.

	1	2	3	4	5	6	7	8	9	10	11	12	13	14	15	16	17	18	19	20	21
Palladium																					
Sobolevskite PdBi														x							
Stibiopalladinite Pd ₅ Sb ₂		x										x	x								x
Vincentite (Pd,Pt) ₃ (As,Sb,Te)																				x	
Zvyagintsevite Pd ₃ Pb							x											x			
Unnamed minerals																					
Pd ₃ Fe		x																			
Cu ₆ Pd																		x			
PdAs ₂	x																				
Unidentified minerals *																					
Pd-Cu	x																				
Pd-Cu-Sb																		x			
Pd-Rh-Sb																					
Pd-Pt-Fe-Cu-Ni			x												x						
Pd-Pt-Cu-Sn-Pb							x														
Pd-Sn														x						x	
Au-Pd							x														
Pd-Te																		x			
Pd-As																		x			
Pd-As-S																				x	
Cu-Pd-Au							x													x	
Pd-Pt-Au																					
Pd oxides							x											x	x		

1 = Bulquiza-Tropoja [18] (Albania); 2 = Kraubath [36] (Austria); 3 = Newfoundland [26], 4 = Thetford mine [24,25] (Canada); 5 = Moa Baracoa [29] (Cuba); 6 = Loma Peguera [21,30] (Dominican Republic); 7 = Pindos [42,45,46], 8 = Othrys [48], 9 = Skyros [41], 10 = Veria [23] (Greece); 11 = Sebuk [59] (Indonesia); 12 = New Caledonia [12,13]; 13 = Osthhammeren [10] (Norway); 14 = Braganca [32] (Portugal); 15 = Nurali [51–53], 16 = Ospa–Kitoi, Khara-Nur [54,55], 17 = Kraka [57] (Russia); 18 = Al'Ays [50] (Saudi Arabia); 19 = Herbeira [35] (Spain); 20 = Berit [49] (Turkey); 21 = Shetland [31,34] (UK). * = PGM without a precise stoichiometry.

The chromitites of Loma Peguera (Dominican Republic), Othrys, Veria (Greece) and Sebuk (Indonesia) contain minerals of Rh and Pt and those of Nurali and Ospa–Kitoi, Khara-Nur and Kraka (Russia) contain minerals of Pt and Pd. The sole presence of Pt minerals has been reported in the chromitites from Moa Baracoa (Cuba) and Skyros Island (Greece) (Table 3 and references therein).

Most of the PPGM described in the ophiolitic chromitites do not occur as isolated inclusions in chromite crystal but are mainly present as irregular and complex grains composed of different ore minerals, including IPGM, base metals (BM) sulfides and alloys. They occur in the altered silicate matrix and in the contact between silicates and chromite. Their size varies from about 1 µm up to exceptionally more than 40 µm. A selection of back-scattered images of the PPGM associated with the PPGE-rich ophiolitic chromitites is presented in Figure 5A–L. Only a few grains of polygonal Pt minerals, about 10 µm in size, were encountered enclosed in chromite in the chromitites from Osthhammeren and Nurali (Table 3 and references therein) (Figure 5A). The PGM reported in the chromitites of Kraubath and Othrys were found only in heavy mineral concentrates, thus information on their textural position is missing.

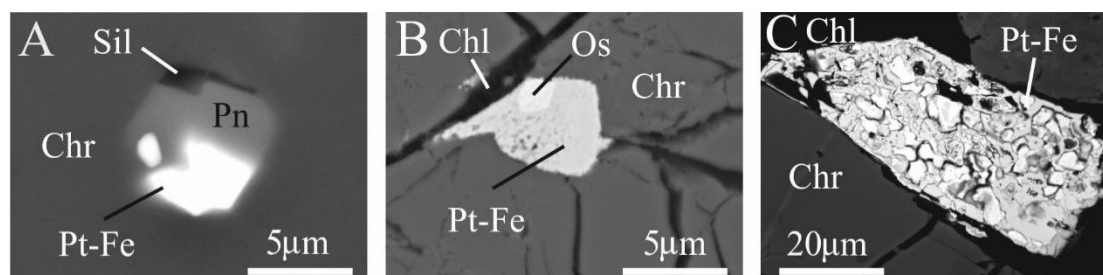


Figure 5. Cont.

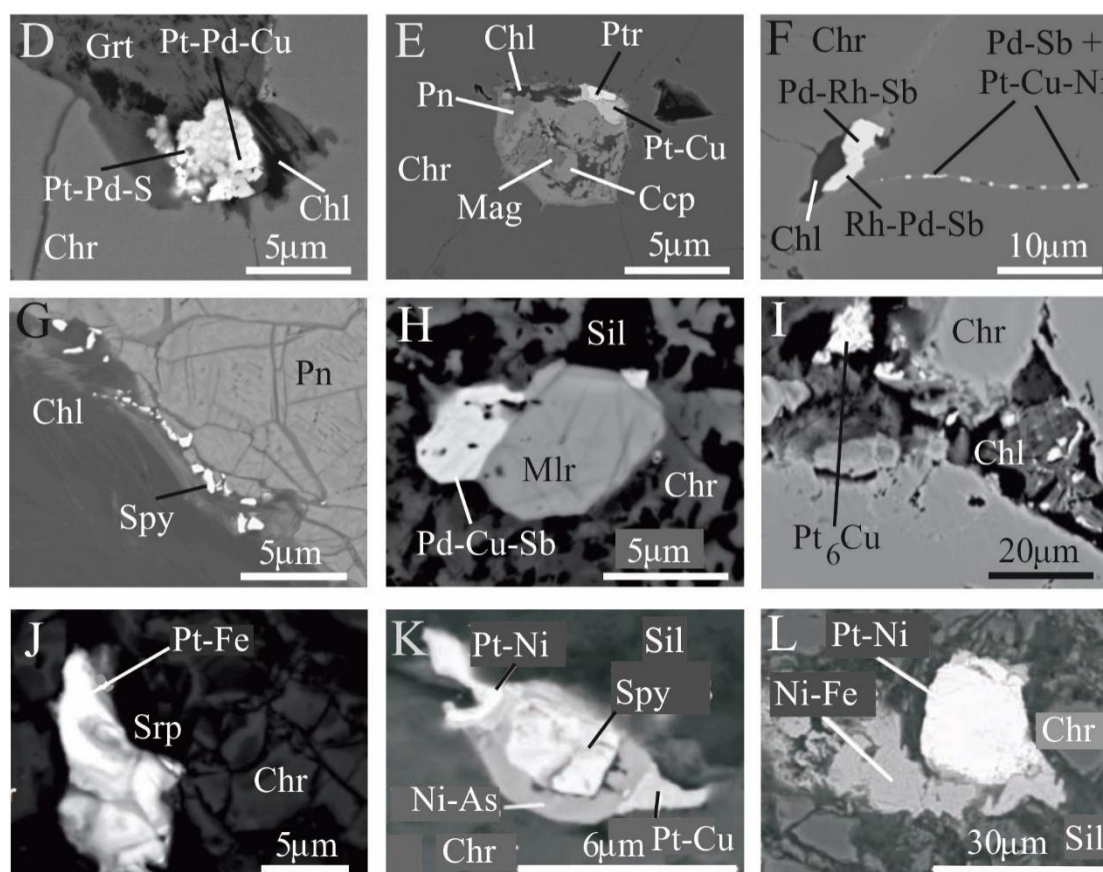


Figure 5. Back-scattered electron images of PPGM from selected the PPGE-rich ophiolitic chromitites. (A) Composite and polygonal inclusion of Pt-Fe alloy, and silicate pyrrhotite in unaltered chromite from Nurali [51]; (B) grain composed of osmium and Pt-Fe alloy in contact with chlorite and chromite from Loma Peguera [21]; (C) Pt-Fe alloy found in the chromitite of Sebuiku showing a porous texture, irregular shape and zoning, in the contact of chromite and chlorite [59]; (D) secondary PGM of Pt-Pd-Cu and Pt-Pd sulfide associated with garnet and chlorite in altered chromite of Nurali [51]; (E) composite grain consisting of potarite, Pt-Cu alloy, pentlandite, chalcopyrite, magnetite and chlorite, in altered chromite of Nurali [51]; (F) altered PGM in contact with chlorite from the Newfoundland chromitites [26]; (G) irregular and tiny grains of sperrylite in the contact between chlorite and pentlandite in the Moa Baracoa chromitites [29]; (H) antimonide of Pd and Cu associated with millerite in contact with altered chromite and silicate of Al'Ays chromitite [50]; (I) secondary Pt_6Cu alloy in the altered matrix of Al'Ays chromitite [50]; (J) Pt-Fe alloy in contact with serpentine found in the Korydallos chromitite [47]; (K) complex grain composed of Pt-Ni, Pt-Cu alloys, sperrylite and Ni-arsenide associated with chromite and altered silicate, Korydallos chromitite [45]; (L) secondary Pt-Ni alloy in contact with Ni-Fe alloy in the altered matrix on the Korydallos chromitite [45]. Abbreviation: Sil = silicates, Chr = chromite, Pn = pentlandite, Pt-Fe = Pt,Fe alloys, Chl = chlorite, Os = osmium, Grt = garnet, Pt-Pd-S = Pt,Pd sulfide, Pt-Pd-Cu = Pt,Pd,Cu alloy, Ptr = potarite, Pt-Cu = Pt,Cu alloy, Ccp = chalcopyrite, Mag = magnetite, Pd-Sb = Pd antimonide, Pd-Rh-Sb = Pd,Rh antimonide, Rh-Pd-Sb = Rh,Pd antimonide, Pt-Cu-Ni = Pt,Cu,Ni alloy, Spy = sperrylite, Pd-Cu-Sb = Pd,Cu antimonide, Mlr = millerite, Srp = serpentine, Ni-As = Ni arsenide, Pt-Ni = Pt,Ni alloy, Pt-Cu = Pt,Cu alloy, Ni-Fe = Ni,Fe alloy.

4.1. Rhodium Minerals

The Rh minerals reported in the overviewed chromitites comprise: (1) sulfides such as bowieite Rh_2S_3 , cuprorhodsitite $CuRh_2S_4$, kingstonite Rh_3S_4 and two unnamed minerals with the composition Rh_2S_3 and Rh_5S_4 , (2) arsenides, i.e., zaccariniite $RhNiAs$, one unnamed Rh_2As and one unidentified Rh-As compound, (3) the sulfarsenide hollingworthite,

(4) the rare antimonide minakawaite RhSb and a compound of Rh-Pd-Sb (Figure 5F) and (5) two unnamed minerals with the formula RhTe and Rh_2SnCu . Bowieite and cuprorhodsite coexist in the chromitites from Bulqiza-Tropoja, Kraubath, Thetford mine and New Caledonia, whereas kingstonite was found only in the Bulqiza-Tropoja-Tropoja samples (Table 3 and references therein). Zaccariniite is the most abundant arsenide and it was found in the chromitites of Newfoundland, Loma Peguera, Veria, Sebuksu Island, Ospa–Kitoi, Khara-Nur and Al'Ays chromitites, whereas the Rh_2As and Rh-As have been reported only from Bulqiza-Tropoja and Al'Ays chromitites, respectively. Hollingworthite is very common, occurring in most of the overviewed chromitites (Table 3 and references therein). On the contrary, minakawaite, the RhTe mineral, and the compound of Rh-Pd-Sb are rare and have been described only from Al'Ays, Bulqiza-Tropoja and Newfoundland occurrences, respectively. The chromitites of Thetford mine, Ospa–Kitoi and Khara-Nur host the potential new mineral Rh_2SnCu (Table 3 and references therein).

4.2. Platinum Minerals

Mineral species of Pt are the most common PGM described in the PPGE-rich chromitites. Pt-bearing alloys occur in all the overviewed samples with the exception of those of Moa Baracoa, Othrys and Skyros Island chromitites (Table 3 and references therein). Among the minerals approved by IMA, the following Pt-bearing alloys have been identified: hongshiite PtCu , isoferroplatinum Pt_3Fe , native platinum Pt , tetraferroplatinum PtFe and tulameenite Pt_2FeCu . An alloy with a composition that approaches the ideal formula $\text{Pt}(\text{Ni,Fe})_3$ has been analyzed in the chromitites of Loma Peguera and Pindos. Another alloy, corresponding to an ideal formula of Pt_6Cu , that approaches the composition of kitagohaite Cu_7Pt (Figure 5I), has also been analyzed in the chromitite of Al'Ays. Pt-alloys containing variable amounts of Pd, Rh, Cu, Ni, Fe and Au and of Ir, Os, Rh, Ni and Fe (Figure 5A–E,I–L) are almost ubiquitous (Table 3 and references therein). They are classified as unidentified minerals because their small size prevents obtaining a precise composition. Sperrylite PtAs_2 is the only Pt-arsenide present in the PPGE-rich ophiolitic chromitites but is abundant when occurring in Kraubath, Pindos (Figure 5K), Newfoundland, Othamneren, Ospa–Kitoi, Khara-Nur, Al'Ays, Herbeira, Berit and Shetland (Table 3 and references therein). Furthermore, sperrylite is the only PGM found in Moa Baracoa (Figure 5G) and Skyros Island chromitites (Table 3 and references therein). The sulfarsenide platarsite PtAsS is less common than sperrylite, being reported only in the chromitites of Bulqiza-Tropoja, Kraubath, Othrys, Veria, Othamneren and Braganca. Mono-sulfides of Pt, characterized by the composition of braggite-cooperite PtS , have been analyzed in the chromitites of Bulqiza-Tropoja, Thetford mine, Pindos, Othrys, New Caledonia, Nurali, Kraka and Herbeira (Table 3 and references therein). One unidentified sulfide of Pt and Pd has been reported in the chromitite of Nurali (Figure 5D). The thiospinel malanite CuPt_2S_4 has been described only in the chromitites from Bulqiza-Tropoja, Thetford mine and New Caledonia (Table 3).

The antimonides genkinite $(\text{Pt,Pd})_4\text{Sb}_3$ and geversite $\text{Pt}(\text{Sb,Bi})_2$ are rare and have been reported in the samples from Shetland and from Ospa–Kitoi, Khara-Nur and Al'Ays, respectively (Table 3 and references therein). Two unidentified oxygenated compounds containing Pt and Pt-Cu have been analyzed in the chromitites of New Caledonia, Herbeira, Berit, Nurali and Al'Ays (Table 3 and references therein).

4.3. Palladium Minerals

Among the Pd-bearing PGM, potarite PdHg (Figure 5E) is the most common, occurring in the chromitites from Bulqiza-Tropoja, Kraubath, Braganca, Ospa–Kitoi, Khara-Nur, Herbeira and Shetland (Table 3 and references therein). Stibiopalladinite Pd_5Sb_2 is also relatively abundant, being present in the chromitites from Kraubath, New Caledonia, Othamneren and Shetland, whereas keithconnite Pd_{3-x}Te has been described only in Bulqiza-Tropoja and Kraubath (Table 3 and references therein). Cabriite Pd_2SnCu , mertierite $\text{II Pd}_8(\text{Sb,As})_3$, paolovite Pd_2Sn , vincentite $(\text{Pd,Pt})_3(\text{As,Sb,Te})$ and zvyagintsevite Pd_3Pb

are rare and occur only in the samples of Thetford mine, Kraubath, Pindos, Berit and Herbeira, respectively (Table 3). The presence of atheneite (Pd,Hg,Pt)As₃, froodite PdBi₂, and sobolevskite PdBi was documented only in the Braganza chromitite. Nielsenite PdCu₃ and skaergaardite PdCu were described in the Korydallos chromitite (Table 3 and references therein). Plumbopalladinite was found only in the Kraka chromitite (Table 3 and references therein). The occurrence of a potential new PGM characterized by the formula Pd₃Fe, probably representing the Pd equivalent of isoferroplatinum, has been reported in the chromitites of Kraubath (Table 3 and references therein). The chromitite from Bulqiza-Tropoja contains an unnamed PGM with the formula PdAs₂ that, on the basis of its chemical composition, can be considered the Pd equivalent of sperrylite. One alloy, Cu₆Pd, has been analyzed in the samples of Al'Ays (Table 3). Palladium also occurs in several unidentified compounds associated with other elements such as Rh, Pt, Au, Cu, Fe, Ni, Sb, Pb, Sn, Te, As, S and O (Figure 5F) (Table 3 and references therein).

5. Discussion

5.1. The PPGE Enrichment in Ophiolitic Chromitites: How Was It Achieved

Although Pt and Pd can circulate through soils in aqueous solutions [63,64], under conditions of partial to complete serpentinization, the PGE are expected to behave inertly [5] and, eventually, to be remobilized only at a small scale [7,19]. Therefore, the effects of low-temperature metamorphism or alteration on the PGE distribution are considered negligible. Most of the overviewed chromitites have been affected by serpentinization to different extents, but their PGE contents have been broadly unaffected, as only redistributions may take place during alteration events, hence the overall PGE compositions represent high-temperature magmatic processes. According to the paper by Barnes et al. [65], the so-called “standard model” was proposed to summarize the hypothesis about the behavior the PGE in mafic and ultramafic melts formulated in the last years. The principles that have been widely accepted and summarized by Barnes et al. [65] are selected and listed in the following.

- (1). The predominant control of the distribution of PGE, being extremely chalcophile under almost all conditions, is the interaction of the magmas with magmatic sulfide liquids [65].
- (2). The partition coefficients of PGE from silicate into sulfide liquids are estimated to range from the order of thousands [65].
- (3). The melting of magmatic sulfides hosted in the mantle source is a critical control of the PGE contents of the resulting melts. The presence of trace amounts of residual sulfide is enough to induce PGE depletion in mantle melts that are sulfide-saturated at source or, alternatively, the degree of partial melting is enough to remove all of the source sulfide and to dissolve it in the silicate melt [65].
- (4). The refractory IPGE are retained in the mantle during partial melting, they decrease in residual melts during fractional crystallization and they are enriched in ultramafic magmatic rocks, independently from the presence of sulfides. On the contrary, the more chalcophile PPGE behave oppositely in the absence of a magmatic sulfide phase [5,65].
- (5). The PGE, under the appropriate conditions, can be fractionated from one another during differentiation or partial melting of sulfide magmas [65]. Pd solubility in silicate melts is orders of magnitude higher than that of other PGE, which may be responsible for Pd depletion of the residual rocks [66–68].

Despite the many factors summarized above, the two main mechanisms controlling the behavior of the PGE during the crystallization of the host chromitite are the partial melting that the mantle source underwent and the crystal fractionation process. Ophiolite complexes represent different oceanic environments characterized by different degrees of partial melting, from low percentages of melting at some mid-ocean ridges (MOR) to higher values in supra-subduction zone (SSZ) complexes [50]. In order to extract all the PGE, including the most refractory, from their mantle source, in which they may occur as alloys and sulfides, high degrees of partial melting, up to 30%, are required [5]. Lower melting degrees between 20 and 25% will dissolve all the preexisting sulfides

leading to PGE liberation, especially the PPGE, into the melts [69]. Most of the mantle-hosted ophiolitic chromitite formed because of the reactions between the residual mantle and percolating magma such as hydrous high-Mg boninitic melts in an SSZ geodynamic setting and the aluminous-rich melt formed in the MOR or in the back arc basin (BAB) environments of the ophiolites [50,70]. The composition of the chromites is related to the nature of the percolating melts, thus most of the Cr-rich chromitites precipitated in the mantle sections of an SSZ ophiolite, whereas Al-rich chromitites are typical of the MOR region. The degree of partial melting of the SSZ mantle is higher than those of the MOR mantle, suggesting that the Cr-rich and Al-rich chromitites should be IPGE- and PPGE-rich, respectively. However, on the basis of available data, this model was successfully applied only to the Bracco chromitite [38]. The PPGE enrichment over IPGE in the Al-rich chromitite of the Bracco ophiolite was explained with the low degree of partial melting of their mantle source. The low degree of partial melting was not high enough to remove all the PGE from the mantle, especially the refractory IPGE. The most incompatible elements, such as sulfur and the PPGE, were partially removed from the mantle, concentrated in the melt and subsequently incorporated in the Bracco chromite forming system [38]. According to Table 1, enrichments in PPGE have been reported in both Cr-rich and Al-rich chromitites; therefore, the model of the low degree of the mantle source as the main factor to control the unusual PGE distribution in the Bracco chromitites cannot be applied to all the overviewed chromitites in this contribution. Melts produced from partial melting of the mantle are either saturated or undersaturated in sulfur. In particular, magmas with boninitic affinity represent sulfur-undersaturated mafic melts, because they derived from a strongly depleted mantle that has lost most, if not all, of its original sulfide phase [69,70]. As a consequence, sulfur saturation is rarely achieved during the precipitation of Cr-rich chromitites hosted in the mantle section of SSZ ophiolite. Examples of these chromitites include those from Kraubath, Newfoundland, Loma Caribe, Veria, Leka, Osthhammeren, Ospa–Kitoi, Khara-Nur, Ulan-Sar’dag, Herbeira and Shetland. For this reason, Escayola et al. [26] proposed that sulfur saturation was achieved also in boninitic magma by reintroduction of sulfur into the residual mantle via metasomatic fluids. On the contrary, tholeiitic magma can be sulfur-saturated [70] and the reaction between this melt and mantle tectonites can be suitable for the precipitation of the chromitite enriched in the more chalcophile PPGE, after the formation of an immiscible sulfide liquid followed by a fractional crystallization process as reported for the Sebuiku chromitite [59] (Figure 3A). The chromitites from Bulqiza-Tropoja-Tropoja, Thetford Mine, Troodos, New Caledonia, Zambales, Al’Ays and some of Kraka occur in the cumulate sequence, above the petrographic Moho, of the host ophiolite, whereas those of Moa Baracoa, Nurali, Berit and very likely also those of Vourinos are located in the MTZ (Table 1 and references therein). The PPGE enrichment in most of these chromites, which are not hosted in the deep mantle, is probably due to the presence of an immiscible sulfide liquid formed from a differentiated melt that, during its migration from the mantle upwards to the MTZ and the cumulus zone, underwent extensive fractional crystallization processes. The original composition of the melt was initially boninitic or tholeiitic and reached the sulfur saturation during its strong differentiation or by assimilation of sulfur from an external source. According to Proenza et al. [28], the local enrichment in PPGE in the chromitite of Moa Baracoa was caused by their interaction with pegmatitic olivine-norite dikes that introduce the PPGE and sulfur to the chromitite originally only enriched in IPGE. The local enrichment of PPGE in the Cliff chromitite of Shetland ophiolite was attributed to a secondary alteration process that was able to upgrade the tenor of PGE [71].

5.2. PGM from the Magmatic Stage to Their Alteration History

Although serpentinization has not significantly changed the PGE content in the overviewed chromitites, the PGM, after their magmatic precipitation, can be altered and transformed by low-temperature hydrothermal fluids. In podiform chromitites, two different occurrences of PGM have been described: (1) tiny and polygonal inclusions in

chromite mainly consisting of Os-Ir-Ru alloys, sulfides such as laurite and erlichmanite and sulfarsenides, namely irarsite and hollingworthite; (2) interstitial PGM at contacts with chlorite and serpentine, generally characterized by an irregular shape and complex mineralogical assemblage, including Os-Ir-Ru alloys and oxides in the IPGE-rich chromitites and a great variety of Rh-Pt-Pd phases in association with Fe-Ni-Cu sulfides and awaruite in the PPGM-rich chromitites. The PGM which are included in chromite crystals are more easily preserved from the alteration processes, whereas the interstitial PGM can be modified by low-temperature secondary hydrothermal fluids and oxidized during weathering. Based on their composition, morphology and mineralogical association, an order of crystallization of the PGM associated with ophiolitic chromitites was suggested. Minerals in the Os-Ir-Ru alloys system, followed by sulfides of the laurite-erlichmanite series and part of the sulfarsenide irarsite and hollingworthite are the first to crystallize at temperatures above or around 1000 °C, prior or concomitantly with the host chromite. The precipitation of these PGM is mainly controlled by the sulfur $f(S_2)$ and arsenic $f(As)$ fugacities in the mantle [16,17,72]. In particular, the $f(S_2)$ during the precipitation of chromitites is expected to increase with decreasing temperature. Although at this stage the sulfur saturation is not achieved, minerals of the laurite-erlichmanite series start to precipitate [16,17,72–74]. The presence of abundant PPGM associated with magmatic Ni-Cu-Fe sulfides occurring in the silicate matrix of the host chromite in the PPGE-rich ophiolitic chromitites can be considered the witness of the presence of an immiscible sulfide liquid during their crystallization. When the magma reaches sulfur saturation, an immiscible sulfide liquid may segregate from the silicate melt, collecting the more chalcophile PPGE available in the system. Therefore, we can argue that the enrichment in PPGE in most of the overviewed ophiolitic chromitites was achieved thanks to the formation of an immiscible sulfide liquid becoming trapped interstitially to chromite crystals at a magmatic temperature, as a consequence of a crystal fractionation process. During the cooling of the PPGE-rich immiscible sulfide liquid, the PPGM start to precipitate together with Ni-Cu-Fe sulfides that may contain PPGE in solid solution as described for the Braganca chromitite [32]. The same model was previously applied to explain the PPGE enrichment in UG2 stratiform chromitites of the Bushveld layered intrusion of South Africa [4], and later also to the Korydallos [45], Al'Ays [50], Newfoundland [26], Nurali [51], Sebuk [59] and Zambales [58] ophiolitic chromitites overviewed in this contribution.

After their crystallization at the magmatic stage, the PPGM and their associated sulfides, being hosted in the silicate matrix of the host chromitite, are more vulnerable to secondary alteration processes [7]. During serpentinization, the magmatic PPGM and Ni-Cu-Fe sulfides underwent desulfurization, generating awaruite and alloys characterized by variable Pt-Pd-Rh-Cu-Ni-Fe assemblages. The occurrence of secondary PPGM containing Sb, As, Bi, Te, Sn, Hg, Pb and Au (Table 3 and references therein) suggests that these elements were originally present in the differentiating magmatic sulfide liquid or, alternatively, they have been introduced by an external source transported by serpentinizing hydrothermal fluids that caused alteration of the host ophiolite [26,71]. Where alteration was most intense, magmatic PGM were transformed to PGE-bearing oxides, which reflects a further alteration stage in the sequence of low-temperature genesis of PGM, as documented in the chromitites from Pindos, New Caledonia, Sebuk, Nurali, Al'Ays, Herbeira and Berit [12,35,45,49,50,52,59]. Despite the evident mineralogical reworking and alteration of the PGM, the data summarized in this contribution suggest that the low-temperature secondary processes that affected the overviewed chromitites caused only a small scale redistribution of PPGE, without changing the whole-rock magmatic PGE contents.

5.3. Are the PPGE- and PPGM-Rich Ophiolitic Chromitites Economic for PGE Recovery?

The PGE are listed among the rare, noble, critical and most valuable metals in nature. Presently, more than 90% of the PGE production comes from two countries, Russia and South Africa. Economically mineable PGE deposits are also found in the layered intrusions of the Great Dyke (Zimbabwe) and Stillwater Complex (USA) as well as in the Sudbury

Basin in Canada [1,2]. PGE production in Russia is dominated by palladium, largely occurring in the Cu-Ni sulfide ore deposits of the Norilsk-Talnakh district, which belongs to the Siberian traps province [75]. The Bushveld layered intrusion in South Africa is known for its large platinum and palladium resources and, according to Cawthorn [1], there are enough PGE reserves to supply world demands for centuries using the current mining techniques. In the Bushveld, the PGE are recovered from three very different ore bodies, namely the Merensky Reef, the UG2 chromitite and the Platreef. Now, the stratiform UG2 chromitites, which extend for nearly the entire 400 km length of the eastern and western limbs of the Bushveld complex, are the only example of chromitites that are mined also for the PGE recovery, being extremely enriched in PPGE. In the UG2 chromitites, the PPGM generally occur associated with sulfides in the interstitial magmatic silicates, and are only rarely enclosed in fresh chromite, similarly to those described in the PPGE- and PPGM-rich ophiolitic chromitites. Although the PGE content may be relatively high, up to 81,867 ppb as detected in one sample from Shetland, presently, the ophiolitic chromitites are not economic considering that: (1) few podiform chromitites are enriched in PPGE and (2) the PPGE enrichment is only local and randomly distributed in chromitites with a small size.

6. Summary and Conclusions

PPGE-rich ophiolitic chromitites are distributed world-wide, but they are rare, representing only the 7% of the investigated podiform chromitites so far. The age of their host ophiolites is variable from Proterozoic to Eocene. They occur at different stratigraphic levels in the ophiolite, i.e., in the mantle, in MTZ and in supra-Moho cumulates. The composition of the host chromite is not an important factor, since in both Cr-rich and Al-rich chromitites an enrichment in PPGE can be achieved.

The main mechanisms that account for the enrichment of the PPGE in ophiolitic chromitites are the high degree of partial melting of the mantle source and subsequent crystal fractionation processes that led to the formation of immiscible sulfide liquid, which collected the available chalcophile PPGE in the system, after the precipitation of their host chromitites.

During cooling of the PPGE-rich immiscible sulfide liquid, the PPGM start to precipitate together with Ni-Cu-Fe sulfides in the silicate matrix of the host chromitite. The PPGM show a great mineralogical variation, including several phases that potentially represent new minerals.

After their crystallization at the magmatic stage, the PPGM and associated sulfides were altered during serpentinization and low-temperature processes and underwent desulfurization, generating awaruite and alloys containing variable amounts of Pt-Pd-Rh-Cu-Ni-Fe. The presence of altered PPGM containing Sb, As, Bi, Te, Sn, Hg, Pb and Au suggests that these elements were originally part of the differentiating magmatic immiscible sulfide liquid or, alternatively, they have been introduced and transported by external hydrothermal and hydrous fluids that caused serpentinization of the host ophiolite. The low-temperature processes that affected the PPGE-rich chromitites were able to modify the original PPGM assemblage without changing the whole-rock magmatic PGE contents.

In spite of the high PGE amounts detected in some samples, presently, the ophiolitic chromitites are not economic for PGE recovery because (1) only a few podiform chromitites are enriched in PPGE and (2) PPGE enrichment is reached only locally and it is randomly distributed in small-size chromitites.

Author Contributions: Conceptualization and data curation, F.Z., M.E.-E., O.K., G.G., B.T., E.P. and A.I.; Bibliographic research, F.Z., M.E.-E., O.K., G.G., B.T., E.P. and A.I.; Writing—original draft preparation, F.Z.; Writing—review and editing, F.Z., M.E.-E., O.K., G.G., B.T., E.P. and A.I. All authors have read and agreed to the published version of the manuscript.

Funding: This research did not receive external funding.

Data Availability Statement: Not applicable.

Acknowledgments: The study of the Uralian ophiolites has been supported to E.P. by Russian State scientific program AAAA-A18-118052590029-6. The authors are grateful to two reviewers for their constructive comments that improved this manuscript and to the editorial staff of Minerals for the professional and fast revision process.

Conflicts of Interest: The authors declare no conflict of interest.

References

1. Cawthorn, R.G. The Platinum Group Element Deposits of the Bushveld Complex in South Africa. *Platin. Met. Rev.* **2010**, *54*, 205–215. [\[CrossRef\]](#)
2. Thormann, L.; Buchspies, B.; Mbohwa, C.; Kaltschmitt, M. PGE Production in Southern Africa, Part I: Production and Market Trends. *Minerals* **2017**, *7*, 224. [\[CrossRef\]](#)
3. Eliopoulos, I.-P.; Eliopoulos, G.; Sfondoni, T.; Economou-Eliopoulos, M. Cycling of Pt, Pd, and Rh Derived from Catalytic Converters: Potential Pathways and Biogeochemical Processes. *Minerals* **2022**, *12*, 917. [\[CrossRef\]](#)
4. Naldrett, A.J.; Von Gruenevaldt, G. The association of PGE with chromitite in layered intrusions and ophiolite complexes. *Econ. Geol.* **1989**, *84*, 180–187. [\[CrossRef\]](#)
5. Barnes, S.-J.; Naldrett, A.J.; Gorton, M.P. The origin of the fractionation of Platinum-group Elements in Terrestrial Magmas. *Chem. Geol.* **1985**, *5*, 303–323. [\[CrossRef\]](#)
6. Garuti, G.; Pushkarev, E.V.; Zaccarini, F. Composition and paragenesis of Pt alloys from the chromitites of the Uralian-Alaskan-type Kytlym and Uktus complexes, northern and central Urals, Russia. *Can. Mineral.* **2002**, *40*, 1127–1146. [\[CrossRef\]](#)
7. Leblanc, M. Platinum-group elements and gold in ophiolitic complexes: Distribution and fractionation from mantle to oceanic floor. In *Ophiolite Genesis and Evolution of Oceanic Lithosphere*; Peters, T.J., Ed.; Kluwer Academic Publ.: Dordrecht, The Netherlands, 1991; pp. 231–260.
8. Stockmann, H.W.; Hlava, P.F. Platinum-group minerals in alpine chromitites from southwestern Oregon. *Econ. Geol.* **1984**, *79*, 491–508. [\[CrossRef\]](#)
9. McElduff, B.; Stumpfl, E.F. Platinum-group minerals from the Troodos ophiolite, Cyprus. *Mineral. Petrol.* **1990**, *42*, 211–232. [\[CrossRef\]](#)
10. Nilsson, L.P. Platinum-group mineral inclusions in chromitite from the Osthhammeren ultramafic tectonite body, South Central Norway. *Mineral. Petrol.* **1990**, *42*, 249–263. [\[CrossRef\]](#)
11. Thalhammer, O.A.R.; Prochaska, W.; Mühlhans, H.W. Solid inclusions in chrome-spinels and platinum group element concentrations from the Hochgrößen and Kraubath ultramafic massifs (Austria). *Contrib. Mineral. Petrol.* **1990**, *105*, 66–80. [\[CrossRef\]](#)
12. Auge, T.; Legendre, O. Platinum-group element oxides from the Pirogues ophiolitic mineralization, New Caledonia; origin and significance. *Econ. Geol.* **1994**, *89*, 1454–1468. [\[CrossRef\]](#)
13. Auge, T.; Maurizot, P. Stratiform and alluvial platinum mineralization in the New Caledonia ophiolite complex. *Can. Mineral.* **1995**, *33*, 1023–1045.
14. Garuti, G.; Zaccarini, F. In-situ alteration of platinum-group minerals at low temperature: Evidence from chromitites of the Vourinos complex (Greece). *Can. Mineral.* **1997**, *35*, 611–626.
15. Melcher, F.; Grum, W.; Simon, G.; Thalhammer, T.V.; Stumpfl, E.F. Petrogenesis of the ophiolitic giant chromite deposits of Kempirsai, Kazakhstan: A study of solid and fluid inclusions in chromite. *J. Petrol.* **1997**, *38*, 1419–1458. [\[CrossRef\]](#)
16. Garuti, G.; Zaccarini, F.; Economou-Eliopoulos, M. Paragenesis and composition of laurite in chromitites of Othrys (Greece): Implication for Os-Ru fractionation in ophiolitic upper mantle of the Balkan peninsula. *Mineral. Depos.* **1999**, *34*, 312–319. [\[CrossRef\]](#)
17. Garuti, G.; Zaccarini, F.; Moloshag, V.; Alimov, V. Platinum-Group minerals as indicator of sulfur fugacity in ophiolitic upper mantle: An example from chromitites of the Ray-Iz ultramafic complex (Polar Urals, Russia). *Can. Mineral.* **1999**, *37*, 1099–1115.
18. Çina, A.; Neziraj, A.; Karaj, N.; Johan, Z.; Ohnenstetter, M. PGE mineralization related to Albanian ophiolitic complex. *Geol. Carpat.* **2002**, *53*, 1–7.
19. Zaccarini, F.; Proenza, J.A.; Ortega-Gutierrez, F.; Garuti, G. Platinum Group Minerals in ophiolitic chromitites from Tehuiztingo (Acatlan Complex, Southern Mexico): Implications for postmagmatic modification. *Mineral. Petrol.* **2005**, *84*, 147–168. [\[CrossRef\]](#)
20. Zaccarini, F.; Garuti, G.; Pushkarev, E.; Thalhammer, O. Origin of Platinum Group Minerals (PGM) Inclusions in Chromite Deposits of the Urals. *Minerals* **2018**, *6*, 108. [\[CrossRef\]](#)
21. Proenza, J.A.; Zaccarini, F.; Lewis, J.F.; Garuti, G.; Longo, F. Platinum Group Element distribution and mineralogy in Loma Peguera chromitites, Loma Caribe peridotite, Dominican Republic. *Can. Mineral.* **2007**, *45*, 631–648. [\[CrossRef\]](#)
22. Tsoupas, G.; Economou-Eliopoulos, M. High PGE contents and extremely abundant PGE-minerals hosted in chromitites from the Vourinos ophiolite complex, Northern Greece. *Ore Geol. Rev.* **2008**, *33*, 3–19. [\[CrossRef\]](#)
23. Tsoupas, G.; Economou-Eliopoulos, M. Transformation of PGM in supra subduction zones: Geochemical and mineralogical constraints from the Veria (Greece) podiform chromitites. *Geosci. Front.* **2021**, *12*, 827–842. [\[CrossRef\]](#)
24. Corrivaux, L.; LaFlamme, J.H.G. Minéralogie des éléments du groupe du platine dans les chromitites de l’ophiolite de Thetford Mines, Québec. *Can. Mineral.* **1990**, *28*, 579–595.

25. Gauthier, M.; Corrivaux, L.; Trottier, L.J.; Cabri, L.J.; Laflamme, J.H.G.; Bergeron, M. Chromitites platinifères des complexes ophiolitiques de l'Estrie-Beauce, Appalaches du Sud du Québec. *Mineral. Depos.* **1990**, *25*, 169–178. [\[CrossRef\]](#)
26. Escayola, M.; Garuti, G.; Zaccarini, F.; Proenza, J.A.; Bedard, J.; Van Staal, C. Chromitite and platinum-group element mineralization at Middle Arm Brook, central Advocate ophiolite complex (Baie Verte peninsula, Newfoundland, Canada). *Can. Mineral.* **2011**, *49*, 1523–1547. [\[CrossRef\]](#)
27. Moring, B.C.; Page, N.J.; Oscarson, R.L. Platinum-Group Element Mineralogy of the Pole Corral Podiform Chromite Deposit, Rattlesnake Creek Terrane, Northern California. In *Geo-Platinum Symposium Volume*; Prichard, H.M., Potts, P.J., Bowles, J.F.W., Cribb, S.J., Eds.; Elsevier: Amsterdam, The Netherlands, 1988; pp. 257–258.
28. Proenza, J.A.; Gervilla, F.; Melgarejo, J.C.; Vera, O.; Alfonso, P.; Fallick, A. Genesis of sulfide-rich chromite ores by the interaction between chromitite and pegmatitic olivine-norite dikes in the Potosí mine (Moa-Baracoa ophiolitic massif, eastern Cuba). *Mineral. Depos.* **2001**, *36*, 658–669. [\[CrossRef\]](#)
29. Proenza, J.A.; Zaccarini, F.; Gervilla, F.; Melgarejo, J.C.; Garuti, G. Platinum group elements mineralogy in sulfide-rich chromitite from Potosí mine (Moa-Baracoa ophiolitic massif, EasternCuba). *Geosciences-Africa* **2004**, *1*, 534–535.
30. Zaccarini, F.; Proenza, J.A.; Rudashevsky, N.S.; Cabri, L.J.; Garuti, G.; Rudashevsky, V.N.; Melgarejo, J.C.; Lewis, J.F.; Longo, F.; Bakker, R.; et al. The Loma Peguera ophiolitic chromitite (Central Dominican republic): A source of new platinum group minerals (PGM) species. *Neu. Jahr. Mineral. Abhandl.* **2009**, *185*, 335–349. [\[CrossRef\]](#)
31. Prichard, H.M.; Tarkian, M. Platinum and palladium minerals from two PGE-rich localities in the Shetland ophiolite complex. *Can. Mineral.* **1988**, *26*, 979–990.
32. Bridges, J.C.; Prichard, H.M.; Neary, C.R.; Meireles, C.A. Platinum-group element mineralization in chromite-rich rocks of Braganca massif, northern Portugal. *Trans. Inst. Min. Metall. (Sect. B Appl. Earth Sci.)* **1993**, *102*, B103–B113.
33. Pedersen, R.B.; Johannesen, G.M.; Boyd, R. Stratiform platinum-group element mineralizations in the ultramafic cumulates of the Leka ophiolite complex, central Norway. *Econ. Geol.* **1993**, *88*, 782–803. [\[CrossRef\]](#)
34. Prichard, H.M.; Ixer, R.A.; Lord, R.A.; Maynard, J.; Williams, N. Assemblages of platinum-group minerals and sulfides in silicate lithologies and chromite-rich rocks within the Shetland ophiolite. *Can. Mineral.* **1994**, *32*, 271–294.
35. Moreno, T.; Prichard, H.M.; Lunar, R.; Monterrubio, S.; Fisher, P. Formation of a secondary platinum-group mineral assemblage in chromitites from the Herbeira ultramafic massif in Cabo Ortegal, NW Spain. *Eur. J. Mineral.* **1999**, *11*, 363–378. [\[CrossRef\]](#)
36. Malitch, K.N.; Melcher, F.; Mühlhans, H. Palladium and gold mineralization in podiform chromitite at Kraubath, Austria. *Mineral. Petrol.* **2001**, *73*, 247–277. [\[CrossRef\]](#)
37. Castroviejo, R.; Moreno, T.; Prichard, H.; Fallick, A. Metalogenia de las ofiolitas de Galicia y unidades asociadas (NW del macizo Iberico, España). In *Complejos Ofiolíticos en Lberoamérica: Guías de Prospección para Metales Preciosos*; Pereira, E., Castroviejo, R., Ortiz, F., Eds.; CYTED: Madrid, Spain, 2004; pp. 231–266, ISBN 9788496023246.
38. Baumgartner, R.J.; Zaccarini, F.; Garuti, G.; Thalhammer, O.A.R. Mineralogical and geochemical investigation of layered chromitites from the Bracco-Gabbro complex, Ligurian ophiolite, Italy. *Contrib. Mineral. Petrol.* **2013**, *165*, 477–493. [\[CrossRef\]](#)
39. Konstantopoulou, G.; Economou-Eliopoulos, M. Distribution of platinum-group elements and gold within the Vourinos chromitite ores, Greece. *Econ. Geol.* **1991**, *86*, 1672–1682. [\[CrossRef\]](#)
40. Economou, M. Platinum-group metals in chromite ores from the Vourinos ophiolite complex, Greece. *Ofoliti* **1983**, *8*, 339–356.
41. Tarkian, M.; Economou-Eliopoulos, M.; Eliopoulos, D. Platinum-group minerals and tetraauricupride in ophiolitic rocks of Skyros island, Greece. *Mineral. Petrol.* **1992**, *47*, 55–66. [\[CrossRef\]](#)
42. Tarkian, M.; Economou-Eliopoulos, M.; Sambanis, G. Platinum-group minerals in chromitites from the Pindos ophiolite complex, Greece. *Neu. Jahr. Mineral. Abhandl.* **1996**, *4*, 145–160.
43. Economou-Eliopoulos, M.; Vacondios, I. Geochemistry of chromitites and host rocks from the Pindos ophiolite complex, northwestern Greece. *Chem. Geol.* **1995**, *122*, 99–108. [\[CrossRef\]](#)
44. Economou-Eliopoulos, M. Platinum-group element distribution in chromite ores from ophiolite complexes: Implications for their exploration. *Ore Geol. Rev.* **1996**, *11*, 363–381. [\[CrossRef\]](#)
45. Prichard, H.M.; Economou-Eliopoulos, M.; Fisher, P.C. Contrasting platinum-group mineral assemblages from two different podiform chromitite localities in the Pindos ophiolite complex, Greece. *Can. Mineral.* **2008**, *46*, 329–341. [\[CrossRef\]](#)
46. Kapsiotis, A.; Grammatikopoulos, T.A.; Tsikouras, V.; Hatzipanagiotou, K.; Zaccarini, F.; Garuti, G. Chromian spinel composition and platinum-group element (PGE) mineralogy of the chromitites from Milia area, Pindos ophiolite complex (NW Greece). *Can. Mineral.* **2009**, *47*, 1037–1056. [\[CrossRef\]](#)
47. Kapsiotis, A.N. Genesis of chromitites from Korydallos, Pindos Ophiolite Complex, Greece, based on spinel chemistry and PGE-mineralogy. *J. Geosci.* **2013**, *58*, 49–69. [\[CrossRef\]](#)
48. Tsikouras, B.; Ifandi, E.; Karipi, S.; Grammatikopoulos, T.A.; Hatzipanagiotou, K. Investigation of Platinum-Group Minerals (PGM) from Othrys Chromitites (Greece) Using Superpanning Concentrates. *Minerals* **2016**, *6*, 94. [\[CrossRef\]](#)
49. Kozlu, H.; Prichard, H.; Melker, F.; Fisher, P.; Brough, C.; Stueben, D. Platinum group element (PGE) mineralisation and chromite geochemistry in the Berit ophiolite (Elbistan/Kahramanmaraş), SE Turkey. *Ore Geol. Rev.* **2014**, *60*, 97–111. [\[CrossRef\]](#)
50. Prichard, H.M.; Neary, C.R.; Fisher, P.C.; O'Hara, M.J. PGE-rich Podiform Chromitites in the Al'Ays Ophiolite Complex, Saudi Arabia: An Example of Critical Mantle Melting to Extract and Concentrate PGE. *Econ. Geol.* **2008**, *103*, 1507–1529. [\[CrossRef\]](#)
51. Zaccarini, F.; Pushkarev, E.; Fershatater, G.; Garuti, G. Composition and mineralogy of PGE-rich chromitites in the Nurali Iherzolite-gabbro complex, southern Urals. *Can. Mineral.* **2004**, *42*, 545–562. [\[CrossRef\]](#)

52. Zaccarini, F.; Garuti, G.; Bakker, R.; Pushkarev, E. Electron Microprobe and Raman Spectroscopy Investigation of an Oxygen-Bearing Pt–Fe–Pd–Ni–Cu Compound from Nurali Chromitite (Southern Urals, Russia). *Microsc. Microanal.* **2015**, *21*, 1070–1079. [\[CrossRef\]](#)
53. Grieco, G.; Diella, V.; Chaplygina, N.L.; Savelieva, G.N. Platinum group elements zoning and mineralogy of chromitites from the cumulate sequence of the Nurali massif (southern Urals, Russia). *Ore Geol. Rev.* **2007**, *30*, 257–276. [\[CrossRef\]](#)
54. Kiseleva, O.N.; Zhmodik, S.M.; Damdinov, B.B.; Agafonov, L.V.; Belyanin, D.K. Composition and evolution of PGE mineralization in chromite ores from the Il’chir ophiolite complex (Ospa-Kitoy and Khara-Nur areas, East Sayan). *Russian Geol. Geoph.* **2014**, *55*, 259–272. [\[CrossRef\]](#)
55. Kiseleva, O.; Zhmodik, S. PGE mineralization and melt composition of chromitites in Proterozoic ophiolite complexes of Eastern Sayan, Southern Siberia. *Geosci. Front.* **2017**, *8*, 721–731. [\[CrossRef\]](#)
56. Kiseleva, O.N.; Airiyants, E.V.; Belyanin, D.K.; Zhmodik, S.M. Podiform chromitites and PGE mineralization in the Ulan-Sar’dag ophiolite (East Sayan, Russia). *Minerals* **2020**, *10*, 141. [\[CrossRef\]](#)
57. Rakhimov, I.R.; Saveliev, D.E.; Vishnevskiy, A.V. Platinum metal mineralization of the South Urals magmatic complexes: Geological and geodynamic characteristics of formations, problems of their genesis, and prospects. *Geodyn. Tectonophys.* **2021**, *12*, 409–434. [\[CrossRef\]](#)
58. Bacuta, G.C., Jr.; Lipin, B.R.; Gibbs, A.K.; Kay, R.W. Platinum-group element abundance in chromite deposits of the Acoje ophiolite block, Zambales ophiolite complex, Philippines. In *Geo-Platinum Symposium Volume*; Prichard, H.M., Potts, P.J., Bowles, J.F.W., Cribb, S.J., Eds.; Elsevier: Amsterdam, The Netherlands, 1988; pp. 381–382.
59. Idrus, A.; Zaccarini, F.; Garuti, G.; Wijaya, I.G.N.K.; Swamidharma, Y.C.A.; Bauer, C. Origin of podiform chromitites in the Sebuiku Island ophiolite (South Kalimantan, Indonesia): Constraints from chromite composition and PGE mineralogy. *Minerals* **2022**, *12*, 974. [\[CrossRef\]](#)
60. Garuti, G.; Pushkarev, E.V.; Thalhammer, O.A.R.; Zaccarini, F. Chromitites of the Urals (part 1): Overview of chromite mineral chemistry and geo-tectonic setting. *Ofioliti* **2012**, *37*, 27–53.
61. Naldrett, A.J.; Duke, J.M. Platinum metals in magmatic sulfide ores. *Science* **1980**, *208*, 1417–1424. [\[CrossRef\]](#)
62. Garuti, G.; Fershtater, G.; Bea, F.; Montero, P.; Pushkarev, E.V.; Zaccarini, F. Platinum-group element distribution in mafic-ultramafic complexes of Central and Southern Urals: Preliminary results. *Tectonophysics* **1997**, *276*, 181–194. [\[CrossRef\]](#)
63. Cook, N.J.; Fletcher, W.K. *Distribution and behaviour of platinum in soils of the Tulameen ultramafic complex, southern British Columbia*; British Columbia Mineral Resources Division (Geological Survey Branch): Vancouver, Canada, 1992; Volume 6, 94p.
64. Cook, N.J.; Wood, S.A.; Yingsu, Z. Transport and fixation of Au, Pt and Pd around the Lac Sheen Cu–Ni–PGE occurrence in Quebec, Canada. *J. Geochem. Explor.* **1992**, *46*, 187–228. [\[CrossRef\]](#)
65. Barnes, S.J.; Mungall, J.E.; Maier, W.D. Platinum group elements in mantle melts and mantle samples. *Lithos* **2015**, *232*, 395–417. [\[CrossRef\]](#)
66. Borisov, A.; Palme, H. Solubilities of noble metals as derived from experiments in Fe-free systems. *Am. Mineral.* **2000**, *85*, 1665–1673. [\[CrossRef\]](#)
67. Mungall, J.E.; Brenan, J.M. Partitioning of platinum-group elements and Au between sulfide liquid and basalt and the origins of mantle-crust fractionation of the chalcophile elements. *Geochim. Cosmochim. Acta* **2014**, *125*, 265–289. [\[CrossRef\]](#)
68. Kuttyrev, A.V.; Kamenetsky, V.S.; Park, J.W.; Maas, R.; Elena, I.; Demonterova, E.I.; Antsiferova, T.N.; Alexei, V.; Ivanov, A.V.; Hwang, J.; et al. Primitive high-K intraoceanic arc magmas of Eastern Kamchatka: Implications for Paleo-Pacific tectonics and magmatism in the Cretaceous. *Earth Sci. Rev.* **2021**, *220*, 103703. [\[CrossRef\]](#)
69. Keays, R.R. The role of komatiitic and picritic magmatism and S-saturation in the formation of ore deposits. *Lithos* **1995**, *34*, 1–18. [\[CrossRef\]](#)
70. Zhou, M.-F.; Sun, M.; Keays, R.R.; Kerrich, R.W. Controls on platinum-group elemental distributions of podiform chromitites: A case study of high-Cr and high-Al chromitites from Chinese orogenic belts. *Geochim. Cosmochim. Acta* **1998**, *677*–688. [\[CrossRef\]](#)
71. O’Driscoll, B.; Garwood, R.; Day, J.; Wogelius, R. Platinum-group element remobilization and concentration in the Cliff chromitites of the Shetland Ophiolite Complex, Scotland. *Mineral. Mag.* **2018**, *82*, 471–490. [\[CrossRef\]](#)
72. Kapsiotis, A.; Grammatikopoulos, T.A.; Tsikouras, B.; Hatzipanagiotou, K.; Zaccarini, F.; Garuti, G. Mineralogy, composition and PGM of chromitites from Pefki, Pindos ophiolite complex (NW Greece): Evidence for progressively elevated fAs conditions in the upper mantle sequence. *Mineral. Petrol.* **2011**, *101*, 129–150. [\[CrossRef\]](#)
73. Bockrath, C.; Ballhaus, C.; Holzheid, A. Fractionation of the platinum-group-elements during mantle melting. *Science* **2004**, *305*, 1951–1953. [\[CrossRef\]](#)
74. Nekrylov, N.; Kamenetsky, V.S.; Savelyev, D.P.; Gorbach, N.V.; Kontonikas-Charos, A.; Palesskii, S.V.; Shcherbakov, V.D.; Kuttyrev, A.V.; Savelyeva, O.L.; Korneeva, A.A.; et al. Platinum-group elements in Late Quaternary high-Mg basalts of eastern Kamchatka: Evidence for minor cryptic sulfide fractionation in primitive arc magmas. *Lithos* **2022**, *412–413*, 106608. [\[CrossRef\]](#)
75. Krivolutsкая, N.; Makvandi, S.; Gongalsky, B.; Kubrakova, I.; Svirskaya, N. Chemical Characteristics of Ore-Bearing Intrusions and the Origin of PGE–Cu–Ni Mineralization in the Norilsk Area. *Minerals* **2021**, *11*, 819. [\[CrossRef\]](#)